COMPENSATING AMPLITUDE DIFFERENCES OF SYNTHETIC APERTURE SONAR IMAGES ACQUIRED AT DIFFERENT FREQUENCIES

B. Lyonnet EXAIL Robotics, France
L. Seyfried EXAIL Robotics, France
M.A. Pinto EXAIL Robotics, France

1 INTRODUCTION

Mine Counter Measures (MCM) operations are often conducted in difficult environments, in shallow water, close to the coast, and with water temperature from 5°C to 35°C. In order to reach the centimetric resolution needed for Automatic Target Recognition (ATR) of mine-like objects of interest, and a high coverage rate of the mine threat area, Synthetic Aperture Sonar (SAS) is the preferred tool[1]. The principle of SAS is to displace a physical antenna through the medium and to integrate multiple successive transmission to create a longer virtual antenna. Array displacement is realized by mounting the antenna on an Autonomous Underwater Vehicle (AUV) or a Towed Vehicle. One of the main challenges of SAS processing is the estimation with a subwavelength accuracy of the platform movement, used by the SAS processing algorithm to reach the desire along track resolution. Estimation errors will lead to defocused images and blurry areas.

Multipath interference can also be a dominant cause of degradation, especially in shallow water[2]. It leads to several degradations such as: ghost targets; a loss in image contrast, with a filling-in of the shadows and finally degradation of bathymetric estimates. All these issues are common to both SAS and legacy sidescan sonars. In particular, shadow of objects on the sea floor is a major feature used in ATR for classification of mines. In addition, multipath affect specifically SAS performance when using data driven method to estimates the platform trajectory, such as Displaced Phased Center Antenna (DPCA) micronavigation[3]. The DPCA technique makes use of the correlation of the sea bottom direct backscatter to estimate the displacement of the SAS between pings and depends critically on a generalized Signal to Noise Ratio (SNR), where the signal is the seafloor backscatter coming from the direct path, while the noise consists of background noise of the sea, system noise, and also multipath interference of various orders, as presented in Figure 1.

In seabed imaging, the main interest is the direct path from the target to the sonar. The interference are the multipath, acoustic rays that bounced one or more times on the sea floor and the sea surface that arrives at the same time instant as the direct path. As a consequence, a classical wide vertical beam sonar on transmitter and receiver will have no possibility to differentiate the direct echo from the multipath.

This effect has been considered in the sonar design of UMISAS, by using two simultaneous frequency bands on two different rows of elements (Figure 1), a VHF row operated at a frequency band centered at 330 kHz and an HF row operated at a band centered at 250 kHz[5], with a bandwidth of 60kHz for an across track resolution of 1.25cm before shading to reduce sidelobes. This design allows for multipath mitigation using narrow beams, exploiting the fact that the multipath arrives or departs at typically greater elevation angles than the direct path. Since each path is travelled in both directions, directivity is required both on transmit and on receive. For the UMISAS 120, the HF antenna, both transmitter and receiver are pointing at long range, with a narrow vertical beam of around 7° at 3dB; whereas the VHF 3dB vertical beam pattern is around 16° and pointing at closer range. Because of the environment geometry, multipath affects more long-range echoes than short ones. The wider VHF beam is oriented downward and is used for short range imaging (typically less than 120 meters). The UMISAS array design is presented in Figure 2. UMISAS design consists of two VHF/HF arrays, the top and the bottom. The bathymetric information is derived from the time delay between both arrays, which informs on the elevation angle of the sea floor.

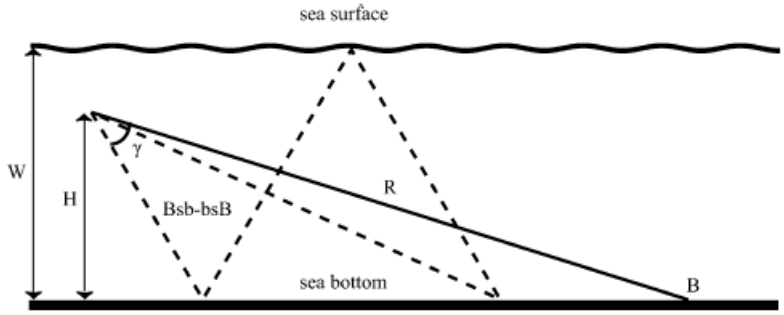

Figure 1 : Illustration of Direct path from sonar to bottom (B) and second order multipath (Bsb, bsB) arriving at the same time[5].

Two SAS images are processed and generated in real time, one for each row, with an overlap area of several meters. For the end user, in MCM context, it is needed to present the two images as one, in a seamless way. The difference in amplitude from one image to the other will decrease the understanding of the overall scene and reduce ATR performance.

The purpose of this paper is the presentation of an embedded algorithm to achieves amplitude compensation at the junction between both images by considering the geometry of the problem, the sonar equation and the detailed knowledge of the antenna system.

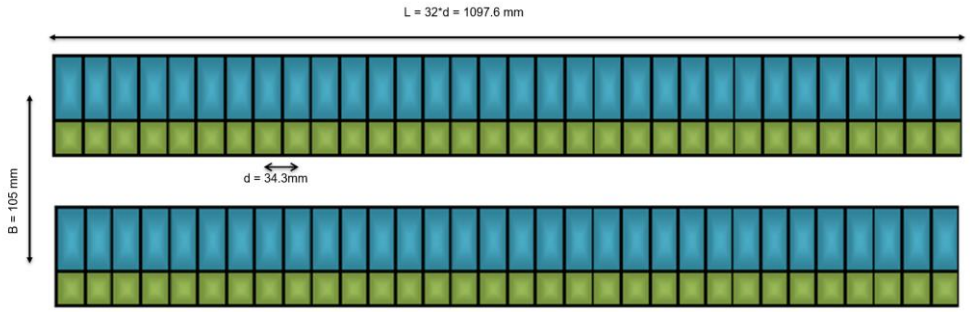

Figure 2 : Dual row UMISAS 120 interferometric array design. HF (250 kHz) receivers in blue, VHF (330 kHz) receivers in green. HF and VHF antennas are oriented downward, with an angle of 5.7 and 14.3 degrees with the horizontal.

The paper is structured as follows. In Section 2, the theoretical amplitude difference between HF and VHF at the junction is explained and the compensation method is developed. In Section 3, experimental results are presented, first on the amplitude correction on one HF image only, then on the entire sonar swath, with images of sea trials done off the coast of Hyères, France, in approximately 30m water depth.

2 AMPLITUDE EXPRESSION

2.1 Sonar equation

Considering the active sonar equation in dB[4], the received power is written as:

$$ER = SL + TS - 2TL + DA$$

With ER the level of the received echoes from the seabed at a receiver element, SL the Source Level, TS the target strength which is dependent of its sound reflectivity, TL the transmission loss, and DA

the vertical Directivity gain of the transmitter and receiver element. These values are all dependent of the frequency of the transmitted signal and will vary from the HF to the VHF element. For transmission losses, we used the classical cylindrical model with medium absorption:

$$2TL = 40\log(R) + 2\,\alpha\,R$$

With R the slant range distance from the center of phase to the target, and α the frequency dependent absorption coefficient. In the context of interface with the sea floor, TS expression is given for a surface backscattering, using Lambert Law. According to the sonar equation, the seamless junction from the HF to the VHF image can be obtained by compensating the amplitude differences. As the UMISAS is composed of two antennas at two different frequencies, the design could be used to increase the maximum range. The source level is 219dB at HF versus 211dB at VHF. As presented in the sonar equation, the SNR is required at long range, where the Transmission Losses are the strongest. To the 8dB difference between HF and VHF, we add 9dB, in water at 25°C, due to the reduction of the sound absorption coefficient from 330kHz to 250kHz. In practice, compensating the SL and TL losses is the simple part of the process.

Before any sea trial, the sonar performances are precisely measured with a calibrated hydrophone in a water tank, a controlled environment, in order to have a clear estimation of SL for each antenna.

2.2 Vertical directivity

The vertical directivity of the receiver element is the source of a major amplitude difference between the VHF and HF rows of elements. The amplitude compensation at the HF/VHF interface should consider the angle of arrival of the acoustic ray on the physical antenna. As the antenna lobe have a strong directivity, especially in HF for multipath mitigation, a slight mistake in the elevation angle could result in major gain correction error. The elevation angle (Figure 3) is affected by the altitude below the sonar at the range of interest and the roll of the AUV during the acquisition. The roll is evolving along the synthetic array, as it is composed of several ping acquired by the moving AUV, which is rotating despite its great stability. Fine roll estimation is obtained through an embedded Inertial Navigation System, the C5, from EXAIL.

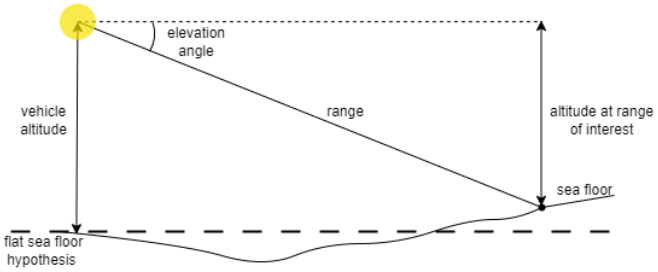

Figure 3: Elevation angle and problem geometry.

Figure 4 is presenting the variation in vertical Directivity gain due to sea floor altitude variations around a vehicle reference altitude of 18m, classical for mine hunting mission with SAS. On the VHF element, the variations are reduced, thanks to the wide opening angle. On the HF antenna, the variation reaches several dB, with a stronger effect at short range as it is the beginning of the main HF beam. As revealed by these calculations, a sea floor variation of a meter could trigger a 3dB difference in amplitude at a range of 100m. Such difference will be visible on the image and should be taken into account.

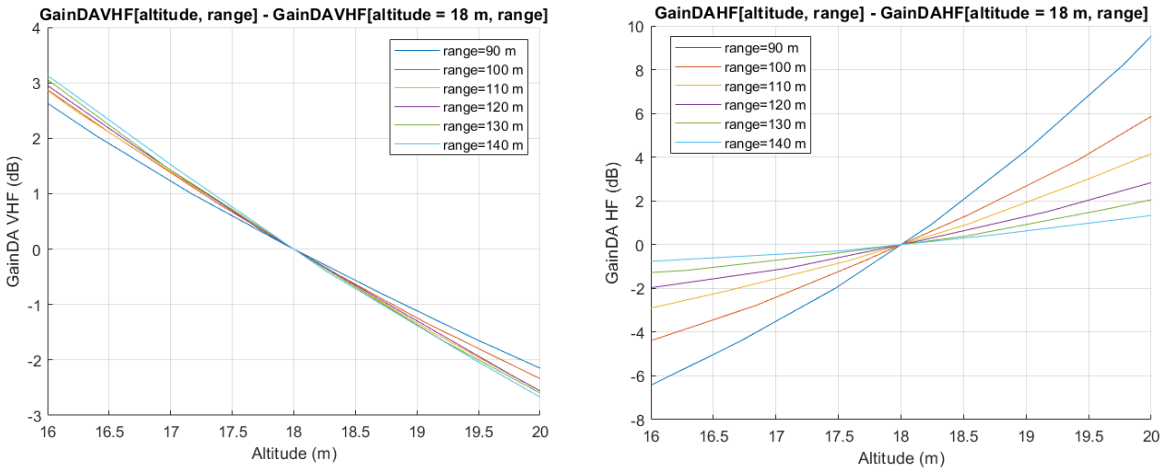

Figure 4: Variation of the directivity gain of the antennas in HF and VHF for a reference altitude of 18m.

From these observations we conclude that an altitude estimation of the HF/VHF junction area should be done, and a flat sea floor approximation is not an acceptable solution. An estimation of the angle of arrival on the antenna is essential for an efficient amplitude compensation.

On this last point, the elevation angle of arrival ϕ is obtained with the UMISAS physical interferometric array, by correlating the received signal on the antennas high and low for each range slices; in what could be consider an algorithm similar to the classical DPCA but apply here on the data from a single ping, registered on two different antennas, high and low. The elevation angle estimated with this method includes variations in altitude at range of interest and roll of the AUV.

The Cramer Rao bound[7] for ϕ angle estimator is:

$$\sigma_\phi = \frac{1}{2\,\pi}\,\frac{\lambda}{b\,\sqrt{BT}}\,\sqrt{\frac{1}{\rho}+\frac{1}{2\,\rho^2}}$$

With λ the wavelength, b the baseline, BT the product between the bandwidth and the signal duration, ρ is the generalized SNR related to the interferometric coherence γ. $\rho = \frac{\gamma}{1-\gamma}$

The major feature for a reliable estimation is an important baseline. In the case of UMISAS, the interferometry on the physical antennas has a high precision thanks to the large baseline of 20 times the wavelength. Elevation angle estimation should be realized for each range slice of the sonar swath[6].

3 RESULTS AND EXPERIMENTS

In October 2023, EXAIL completed a series of sea trial near Hyères, France, with the UMISAS installed on the AUV A18M developed by EXAIL. One of the many challenges of the image realization is the time synchronization, as asynchronous HF and VHF transmission will result in images covering different areas. Seamless mosaicking will still be possible but with a more complicated and cumbersome process and is not the solution retain here. Another source of error is the time synchronization of Sonar and INS data, as vehicle orientation is used by the DPCA algorithm for micronavigation and movement estimation. UMISAS is taking advantage of the state-of-the-art A18M INS to have a high-level orientation estimation, allowing for a robust and precise SAS processing.

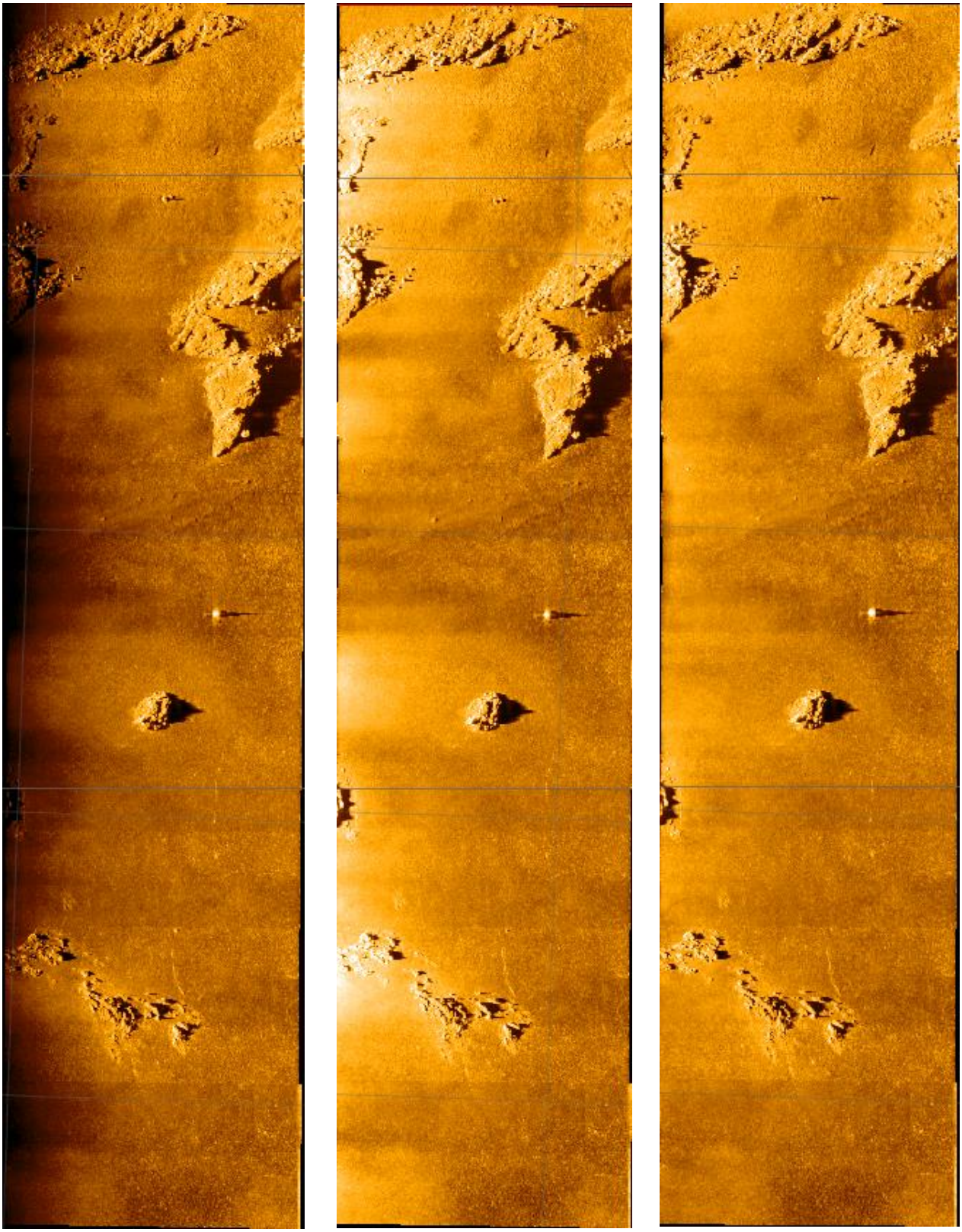

Figure 5: Mosaic (3 cm) at starboard with HF band (dB range 8-28), no gain correction (left), with antenna gain correction and flat sea floor hypothesis (middle), with antenna gain correction and altitude correction through DPCA intra (right).

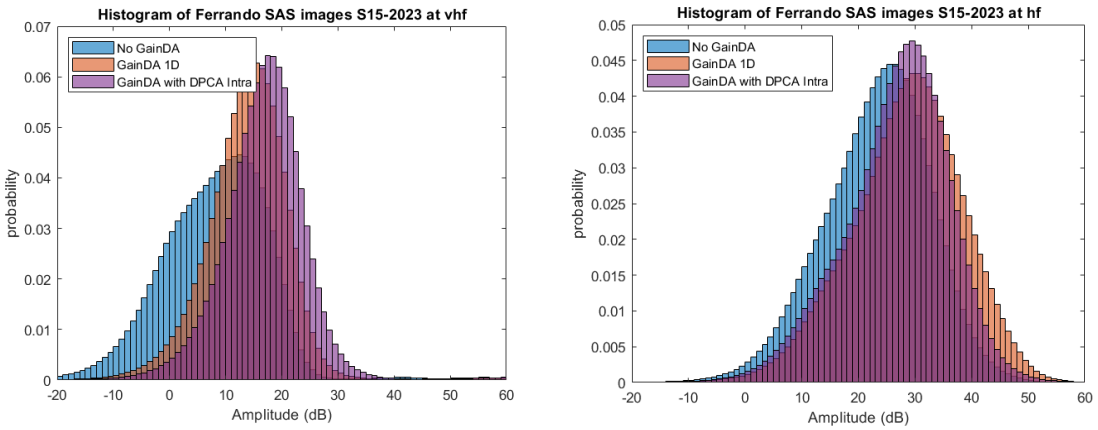

Figure 6: histogram of the VHF and HF antenna SAS images, without gain correction, with antenna gain correction and flat sea floor hypothesis and with antenna gain correction taking into account roll and altitude correction through DPCA intra calculated at the junction range of HF/VHF.

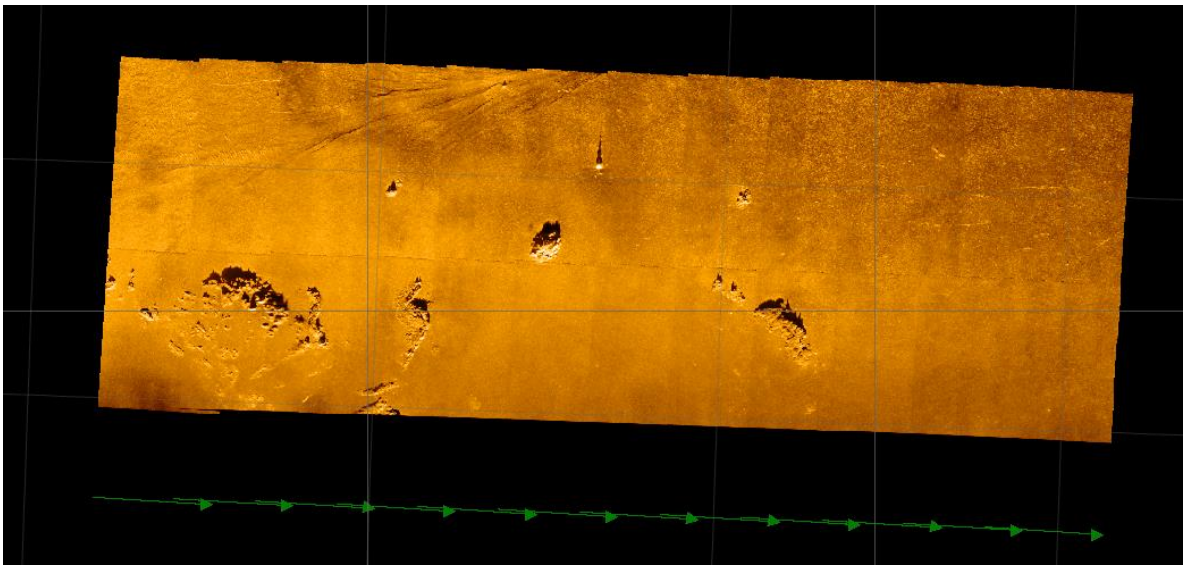

Figure 7: port SAS images VHF and HF band (dB range 5-25) with antenna gain correction and altitude correction through DPCA intra. Extract from UMISOFT DM Map software. 600 meters along track, from 30m to 170m across track

In Figure 5, we present the results of the amplitude compensation on the HF mosaics, composed of several UMISAS tiles, at different steps. The left image is with the correction of the two ways Transmission loss only, without Antenna Gain Correction, but still with residual amplitude variation from the roll of the vehicle. We observe image amplitude variations in across-track and along-track. In across-track, these variations can be attributed to the antenna directivity. In along-track, these variations are modulated by vehicle roll and seabed altitude (rocky areas). The middle image is with a simple Antenna Gain correction, with a flat seabed hypothesis and a vehicle altitude of 18 m. This Gain correction increases the amplitude in the image at short range. Along-track modulations are still

visible. The right image present last step of the amplitude correction algorithm, with a correct Antenna Gain correction, using the elevation angle estimation obtained through the physical antenna interferometry. Elevation angle estimation includes variations due to vehicle roll and seabed altitude. The last image shows a great improvement from the non-compensated image, with objects of the same nature and at different distance displaying a consistent Target Strength. In particular, the seabed features at short range, where the vertical directivity have a strong variation, is correctly compensated by considering the local elevation angle in the last step of our method. These results are confirmed by the histogram of the generated image, as displayed in Figure 6. As it could be expected, the compensated image is presenting a sharper histogram, more representative off the sea floor structure. Shadows and strong echoes from rocks and humans clutter are the only component stepping out of the main curve.

Figure 7 presents the full swath HF/VHF SAS image, with a seamless junction. It is worth noting that the VHF centers of phase are slightly lower than the HF ones, provoking a small bias between the two generated image at the junction in across track. This is taken into account by translating the slant range VHF image by a fixed value dependent of the HF to VHF antenna distance, and the slant range of the junction. For UMISAS, with a HF/VHF distance of 40mm, the bias is of less than a pixel size in across track.

4 CONCLUSION

In this paper, a method is presented to compensate the amplitude difference between two SAS images created from two antennas at different frequencies mounted on the same platform. We demonstrate the importance of altitude and angle of arrival estimation with a fine precision for a coherent amplitude compensation of the Antenna Gain. Future work should focus on creating a calibrated SAS, allowing for a clear TS estimation.

5 REFERENCES

1. M. A. Pinto, B. Lyonnet, T. Simian, & S. Meltzheim. *A New High Resolution AUV-Based Synthetic Aperture Sonar for Challenging Environmental Conditions.* In OCEANS 2023-MTS/IEEE US Gulf Coast (pp. 1-5). IEEE (2023, September).
2. R. E. Hansen, H. J . Callow, T. O. Sæbø, S. A. Synnes, P. E. Hagen, T. G . Fossum, & B. Langli. *Synthetic aperture sonar in challenging environments: Results from the HISAS 1030.* Proceedings of Underwater Acoustic Measurements (2009).
3. A. Bellettini, & M. A. Pinto, *Theoretical accuracy of synthetic aperture sonar micronavigation using a displaced phase-center antenna.* IEEE journal of oceanic engineering, 27(4), 780-789 (2002).
4. X. Lurton. *An introduction to underwater acoustics: principles and applications*. Springer Science & Business Media (2002).
5. A. Bellettini, & M.A. Pinto, *Design and experimental results of a 300-kHz synthetic aperture sonar optimized for shallow-water operations*. IEEE Journal of oceanic engineering, 34(3), 285-293 (2008).
6. S. A. Synnes, R. E. Hansen, & T. O. Sæbø, *Assessment of shallow water performance using interferometric sonar coherence.* Proceedings of Underwater Acoustic Measurements, 6. (2009)
7. D. Billon, *About accuracy of the elevation angle measurement in interferometric synthetic aperture sonar.* In Europe Oceans 2005 (Vol. 1, pp. 650-654). IEEE. (2005, June)